Eur. Phys. J. A **13**, 149–154 (2002)

THE EUROPEAN PHYSICAL JOURNAL A

© Società Italiana di Fisica
Springer-Verlag 2002

Influence of entrance channel properties on heavy-ion reaction dynamics

D.J. Hinde, A.C. Berriman, R.D. Butt, M. Dasgupta, C.R. Morton, A. Mukherjee, and J.O. Newton

Department of Nuclear Physics, R.S.Phys.S.E., Australian National University, ACT 0200, Australia

Received: 1 May 2001

Abstract. In the fusion of heavy nuclei, there is a distribution of fusion barrier energies resulting from coupling between intrinsic motion and internal degrees of freedom. Precise experimental measurements of excitation functions have allowed the extraction of the distributions by taking the second derivative using a point-difference method. In the case of statically deformed nuclei, experimental data shows that the different fusion barrier energies correspond to different physical configurations of the colliding nuclei, the latter affecting the subsequent dynamical trajectories over the potential energy surface, influencing the ultimate reaction products, as for example in quasi-fission. The fusion barrier distribution is also valuable in understanding the fusion of weakly bound nuclei, enabling a reliable prediction of the expected fusion cross-sections, and thus the determination of fusion suppression factors at above-barrier energies.

PACS. 25.70.Jj Fusion and fusion-fission reactions

1 Introduction

One of the important applications of radioactive ion beams will be to form, through nuclear fusion, new nuclei far from stability. Studies of fusion of radioactive nuclei should result in insights into the properties of the radioactive nuclei undergoing fusion, as well as into the fusion process itself. It is important to strive to obtain precise and accurate cross-sections in such measurements, as results for reactions with stable beams discussed below demonstrate the value of such data.

The fusion barrier distribution represents the probability that a fusion barrier will be found at a given beam energy, and its existence can be most easily appreciated in the case of fusion with a statically deformed nucleus. In the decade since the first proposal [1] that a representation of the fusion barrier distribution could be extracted by taking the second derivative of the fusion excitation function, considerable development in our quantitative understanding of the fusion of heavy nuclei has occurred [2], both from an experimental and a theoretical point of view; the latter partly due to the demands placed on theory by the new, precise fusion data which have been obtained.

For nuclei with a charge product greater than about 250, it has been found that the width of the fusion barrier distributions is typically more than 5% of the mean barrier energy. By appropriate choice of colliding nuclei, barrier distributions characteristic of the excitation of different collective modes of the colliding nuclei have been observed. These include rotational modes [3] (which classically correspond to a static deformation) and vibrational modes (both surface octupole [4] and quadrupole [5] vibrations). Small effects of the single-nucleon transfer have also been isolated [4]. Correlations have been made betweeen large changes in the shape of the barrier distributions (enhancing the sub-barrier fusion by many orders of magnitude) and the presence of positive Q-value multi-neutron transfers [6]. The latter may be related to the classical concept of neck formation.

It can be expected that in the fusion of radioactive nuclei, the excitation of such collective modes strongly coupled to the relative motion will also have the largest influence on fusion. Because of the different N/Z ratios of radioactive species, multi-nucleon transfers may have a large and favourable effect in particular cases. However, the weakly bound nature of *light* radioactive nuclei could be expected to result in a suppression of fusion due to their breakup in the field of the target nucleus before the fusion barrier is reached. Already, fusion excitation functions have been measured for radioactive species, (see, for example, contributions from C. Signorini and J.J. Kolata in these proceedings) and intriguing results are being obtained. In understanding these results, comparisons with their stable cousins is important, to isolate the effects which are due to exotic N/Z ratios. In this regard, fusion studies of weakly bound stable nuclei such as ^{6,7}Li and ^{9}Be give valuable complementary information, since at present, more extensive data can be obtained for such nuclei.

Details of fusion measurements made at the Australian National University, for these nuclei will be presented, and conclusions given, after the influence of the entrance chan-

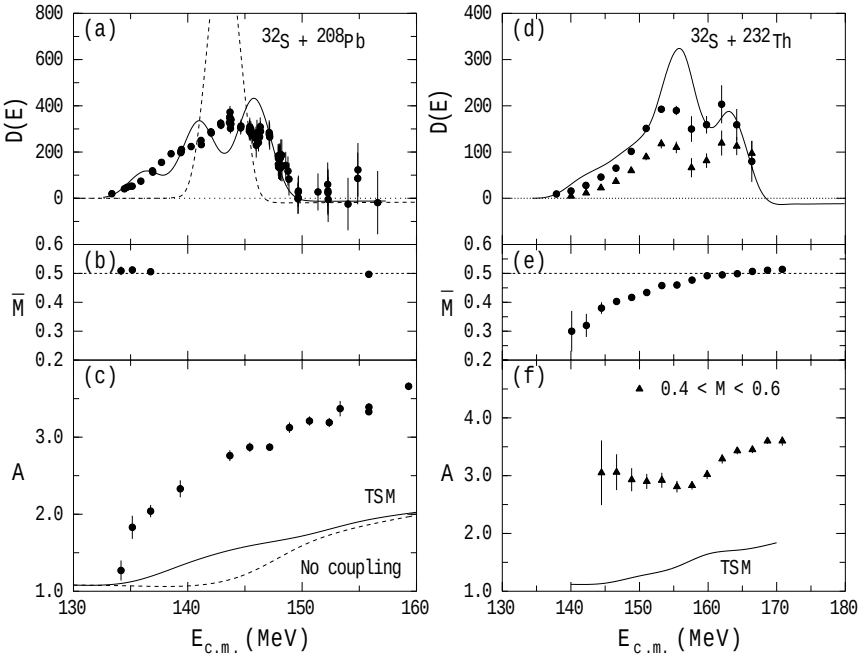

Fig. 1. (a) The barrier distribution for ^{32}S + ^{208}Pb together with (b) the centroids of the fission mass splits (symmetric fission is indicated by the dashed line) and (c) the energy dependence of the fission anisotropy. The predictions of the TSM with and without the inclusion of couplings in fusion are given by the dashed and full lines, respectively. Similar quantities for ^{32}S + ^{232}Th are shown in (d), (e) and (f), the results for symmetric mass splits between 0.4 and 0.6 of the compound-nucleus mass being indicated by triangles. In both reactions, the calculated fusion barrier distributions are not best fits, but demonstrate that the inclusion of wide barrier distributions does not allow reproduction of the measured A values.

nel properties on fission is discussed. The latter subject is important if radioactive nuclei are to be used to try to form superheavy nuclei which are closer to the predicted island of stability than can currently be accessed. This is because entrance channel effects can have a dramatic influence on the competition between compound-nucleus formation and the quasi-fission process. To form superheavy nuclei, of course the former process needs to be optimised.

2 Effect of static deformation on fusion-fission and quasi-fission competition

Generally, different fusion barriers correspond to different conditions or configurations of the two nuclei at the fusion barrier radius. Does the configuration at fusion influence the outcome of the reaction? If an equilibrated compound nucleus is formed, according to Bohr's independence hypothesis, the answer should be no. If, however, this is not the case, as in quasi-fission, some influence of the configuration at fusion could remain. An investigation of the influence of fusion barrier energy and configuration on the subsequent fission process has been carried out for reactions involving both spherical and statically deformed heavy nuclei. It is crucial to appreciate that the range of fusion barrier energies encountered can be controlled by choosing the bombarding energy within the range of the fusion barrier distribution [7,8]. At low energies, only the low fusion barriers result in capture, whilst above the fusion barrier region, all fusion barriers contribute to the yield.

By comparing the measured fission properties (in particular angular distributions) as a function of the beam energy with calculations using the statistical transition state model (TSM) [9], which should be able to describe the fusion-fission process, changes in the fission dynamics can be investigated.

The principal variables determining the fission angular distributions (usually characterised by the anisotropy A, defined as the ratio of the yield at 0° or 180° to that at 90°) are shown by the approximate expression for A based on the TSM:

$$A = W(180^\circ)/W(90^\circ) \approx 1 + \frac{\langle J^2 \rangle}{4K_0^2} = 1 + \frac{\langle J^2 \rangle \hbar^2}{4T\mathcal{J}_{\rm eff}}. \quad (1)$$

Thus A is sensitive to the mean square angular momentum leading to fission $\langle J^2 \rangle$, as well as to the variance K_0^2 of the distribution of K (the projection of J onto the fission axis) centred at $K = 0$. Within the TSM, K_0^2 is determined by the product of the temperature T at the fission saddle-point, and the effective moment of inertia $\mathcal{J}_{\rm eff}$ associated with the saddle-point shape. Fusion models fitting experimental data are used to determine $\langle J^2 \rangle$ [10], whilst T and $\mathcal{J}_{\rm eff}$ are determined from the statistical model and the rotating finite range model [11] (RFRM), respectively. One characteristic of quasi-fission is the small values of K_0^2 (large A), which in general terms can be related to failure to form a *compact* compound nucleus.

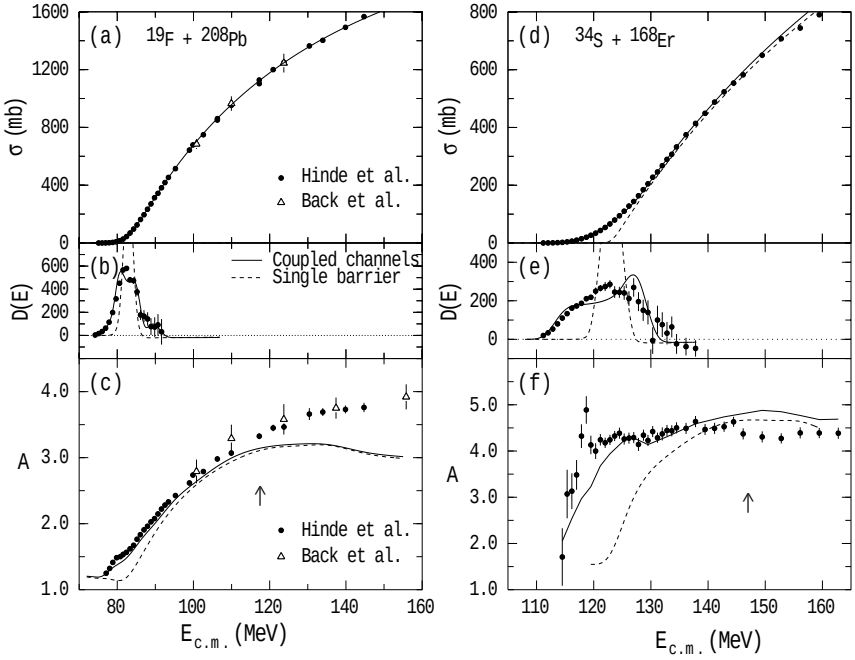

Fig. 2. The fusion excitation function (a), barrier distribution $D(E)$ (b), and fission anisotropies (c), for the reaction ^{19}F +^{208} Pb, together with calculations of all three quantities based on the assumption of a single fusion barrier (dashed lines) and for a coupled-channels fusion calculation which reproduces the fusion data (full lines). The same quantities are shown for ^{34}S with ^{168}Er in panels (d), (e) and (f). The arrows indicate the lowest energies for each reaction at which a significant fraction of fission events result from systems where the fission barrier is less than the temperature. As the energies increase, this fraction increases.

To investigate experimentally the effect of static deformation, the two reactions ^{32}S + ^{208}Pb (spherical) and ^{32}S + ^{232}Th (deformed) are compared. It was known that there is a substantial quasi-fission yield for both reactions from anisotropies for the same [12] or similar reactions [13]. Recent measurements at the ANU have mapped out the detailed behaviour of the fission properties across the fusion barrier energy region. Figures 1(a),(d) show the barrier distributions, (b),(e) the centroids of the fission mass distributions measured at a backward angle, and (c),(f) the anisotropies as a function of beam energy for each reaction. In both cases, the calculated anisotropies labelled TSM are small, whether the width of the barrier distribution is included (full lines) or not (dashed line), because the RFRM saddle-point shapes are very compact for such fissile compound nuclei.

For both reactions, the measured A lie well above the calculations, indicating that the K-distributions are narrow. This implies that compact shapes are not generally reached in these reactions, consistent with previous conclusions [12,13] that quasi-fission predominates. The energy dependence of A for the two reactions is, however, very different. For ^{32}S + ^{232}Th, A rises as the energy falls below the average fusion barrier energy. This feature has also been observed for lighter projectiles incident on deformed heavy targets, for example ^{16}O + ^{238}U [8]. There, it was proposed that fusion at the lowest beam energies, which results exclusively from the projectile approaching the tips of prolate deformed target nuclei, leads preferentially to quasi-fission. This hypothesis is supported by the energy dependence of the fission mass distributions for ^{32}S + ^{232}Th, which show a marked change in shape and centroid, as indicated in fig. 1(e). For ^{32}S + ^{208}Pb, however, the anisotropy falls monotonically with energy, and the mass distributions show no dramatic change in shape or centroid, unlike those for the ^{232}Th target. Thus there is no indication in the data of a change in the character or probability of quasi-fission which is dependent on the energy of the barrier encountered, for this reaction. This is most likely correlated with the high frequency of the vibrational excitations of ^{208}Pb, as opposed to the low frequency associated with collective rotational excitations of ^{232}Th. In reactions involving heavy deformed nuclei, the configuration found at the fusion barrier is thus likely to remain essentially unchanged up to the time the two nuclei start to merge together (closer than the fusion barrier configuration) and so can influence the subsequent fission dynamics. For vibrational nuclei, a configuration resulting in a low-energy fusion barrier will not necessarily translate into an elongated composite nucleus, due to the high frequency of the relevant collective modes.

The energy dependence of the fission behaviour in these two reactions, as well as for reactions of lighter projectiles with deformed actinides (such as ^{16}O + ^{238}U [8]) thus points to the unique influence of static deformation of the heavy nucleus on the subsequent reaction dynamics, as opposed to an effect simply due to elongation at the fusion barrier configuration. Recent data on evaporation residue formation probabilities for reactions of heavy projectiles with statically deformed target nuclei [14,15],

show a dramatic suppression of residues at sub-barrier energies, consistent with competition between fusion-fission and quasi-fission depending on the fusion barrier configuration, as suggested in refs. [7,8].

3 Effect of static deformation on fission at high angular momentum

At high angular momentum, the TSM is expected to lose its validity [16,17]. This occurs because as J increases, the fission barrier height $E_{\rm f}(J)$ is reduced, ultimately to zero, and here the symmetric fission saddle-point shape can no longer be defined. Fission from such high angular momenta where the fission barrier is no longer significant is called fast fission [18,19].

Without the controlling influence of the saddle-point, can fast fission be modelled in a simple way, and is it influenced by static deformation, as is quasi-fission? An obvious problem in studying the latter question is that beam energies above the fusion barrier region are required in order to introduce high angular momentum, and thus the full range of fusion barriers will always be encountered.

To investigate these questions, firstly the reaction ^{19}F + ^{208}Pb (spherical) was studied in detail, from below to 1.7 times the fusion barrier energy [20]. TSM calculations which describe well the A values at low energies (see fig. 2(c)), fail at higher energies, the calculated A values ultimately decreasing with increasing energy to lie well below the measured values. This fall is due to the RFRM predicting increasingly compact saddle-point shapes for higher J, as the fission barrier height approaches zero. It has been shown [20] that the monotonic rise of the data can be explained by eliminating the controlling influence of the saddle-point shape (which is used in the TSM description) at angular momenta where $E_{\rm f}(J) \leq T$, rather than where $E_{\rm f}(J) = 0$, consistent with simple expectations and dynamical calculations [21]. The beam energy above which a significant fraction of fission events have $E_{\rm f}(J) \leq T$, is indicated by the arrow in fig. 2(c).

The high-energy (angular momentum) data require a smaller value of K_0^2 than predicted using the RFRM saddle-point shapes. This could be explained by postulating an equilibrium distribution of K associated with the most compact shape attained during the reaction, which must be more elongated than the saddle-point shape. Alternatively, the small K_0^2 can be thought of as resulting from the failure to reach an equilibrium K-distribution, implying a memory is retained of the K-distribution in the entrance channel [22]. The principal axis of the entrance channel configuration in this reaction is along the line joining the mass centres, which in turn is normal to the angular momentum vector, as illustrated in fig. 3(a). Ignoring the ground-state spin (1/2) of ^{19}F, the entrance channel K is thus zero. A memory of the entrance channel K-distribution would lead to a smaller K_0^2 than predicted by the TSM.

To distinguish between these two explanations, a measurement of fast fission was carried out for the reaction

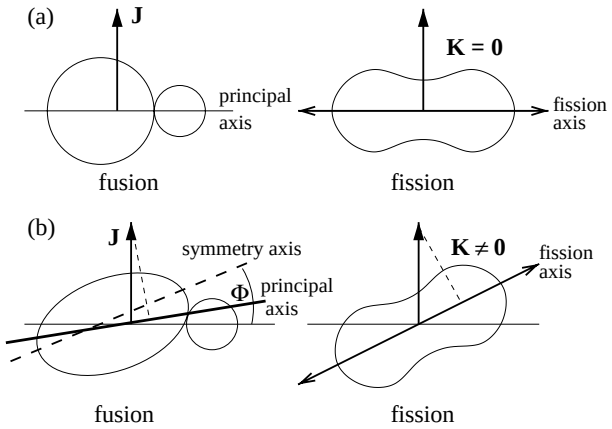

Fig. 3. (a) Fusion of a spherical projectile with a spherical target nucleus produces a K-distribution in the entrance channel that is a delta function at $K = 0$, since the principal axis of the combined system is always perpendicular to the plane containing the angular momentum vector **J**. (b) Fusion with a deformed target nucleus, at an angle Φ to its nuclear symmetry axis (dashed line), forms a principal axis (thick solid line), which gives rise to a non-zero K-distribution in the entrance channel. If the system fission along the "pre-formed" elongation axis, then a K-distribution wider than that for the spherical system can result.

^{34}S + ^{168}Er [23], where ^{168}Er has a large static quadrupole deformation of $\beta_2 = 0.34$. The experimental results are shown in fig. 2, (d)-(f), compared with TSM calculations as for ^{19}F + ^{208}Pb. At energies below the average barrier, the calculated and measured A's are not in extremely good agreement. This could be a dynamical effect, or may be due to the high sensitivity of the calculations at these energies to the fusion angular momentum distribution, as illustrated in fig. 2(f) by the difference between the full and dashed lines. At higher energies, this sensitivity is clearly much reduced. In contrast with the ^{19}F + ^{208}Pb reaction, at high energies (angular momenta) the measured A values are *smaller* than those calculated, implying a *wider* K-distribution than predicted by the TSM. This cannot be explained in terms of equilibrium at a more elongated shape than the RFRM saddle-point, but can be qualitatively related to a memory of the entrance channel configurations [24] as described below.

Suppose the projectile at contact makes an angle Φ to the symmetry axis of the deformed target nucleus, as illustrated in fig. 3(b) (at these high bombarding energies, all angles will lead to fission). The angular momentum brought in by the projectile is perpendicular to the line joining the mass centres, whilst the principal axis of the system lies at an angle between the symmetry axis of the deformed target nucleus and the line joining the mass centres. This can be thought of as an elongation axis "preformed" in the fusion process, and the K-value on this axis can be large. Fission, which is a diffusive process, may occur more readily along this axis, or along the symmetry axis of the target nucleus [25,26]. In either case, a broader K-distribution will be found than for a spheri-

cal target nucleus. These high-J trajectories, which should never reach the compact equilibrium shape according to the ^{19}F + ^{208}Pb data, can thus have a K-distribution whose variance is *greater* than the TSM value, resulting in a smaller anisotropy, explaining the experimental results for ^{34}S + ^{168}Er shown in fig. 2(f).

Evidence has been presented that fast fission favours the elongation axis pre-formed in the fusion process. Thus in fast fission as well as in quasi-fission, static deformation in the entrance channel appears to influence the dynamics of the subsequent evolution of the system over the potential energy surface.

4 Breakup of weakly bound nuclei

Unambiguous determination of the mean fusion barrier allows the prediction of the fusion cross-sections at above-barrier energies, which, as shown in fig. 2, (a) and (d), agree well with experimental data in the case of strongly bound projectiles. Our concept, first presented in refs. [2, 27], was to apply this prodedure to reactions with weakly bound nuclei, the ratio between the measured and calculated cross-sections then giving a direct measure of the suppression of fusion due to breakup.

Measurement of the yields of heavy residues was accomplished by detecting their ground-state or isomeric decay α-particles, firstly for the ^{9}Be + ^{208}Pb reaction [2, 27], and more recently for the ^{7}Li + ^{209}Bi reaction [28]. Alpha-particles from nuclei with $Z = 86, 85, 84$ were observed, and cross-sections determined. By making measurements for two calibration reactions, ^{13}C + ^{204}Hg and ^{18}O + ^{198}Pt, forming the same compound nuclei as in the above reactions, it was found that only residues with $Z = 86$ (Rn) were produced, together with a small fission yield. This indicated that the $Z = 85, 84$ nuclei must result from the breakup of the projectiles, followed by fusion of one of the fragments with the target nucleus.

The complete fusion cross-sections for the ^{7}Li + ^{209}Bi and ^{9}Be + ^{208}Pb reactions were thus defined as the sum of the Rn xn evaporation residue cross-sections and the fission cross-section at each beam energy, and are shown in fig. 4, (a) and (b), whilst the experimental barrier distributions, $\mathrm{d}^2(E\sigma_{\mathrm{fus}})/\mathrm{d}E^2$, determined from the fusion excitation functions using a point difference formula, are shown in fig. 4, (c) and (d). The average barrier positions obtained from the experimental barrier distributions for ^{7}Li + ^{209}Bi and ^{9}Be + ^{208}Pb are 29.6 ± 0.4 MeV and 38.3 ± 0.6 MeV, respectively.

Realistic coupled-channels calculations [28] were made choosing a nuclear potential which reproduced the measured average fusion barrier energy. Couplings to states in projectile and target were included. The cross-sections and barrier distributions are shown in fig. 4 by the dashed lines. They give significantly higher cross-sections than are observed. Agreement between the measured and calculated quantities can be achieved if the calculated fusion cross-sections are scaled by 0.73 and 0.68 for the ^{7}Li and ^{9}Be induced reactions, respectively. The result of such a scaling is shown by the full lines in fig. 4. This scaling factor will be model dependent at the lowest energies, as the calculations are sensitive to the types of coupling and their strength. However, at energies around and above the average barrier, the scaling factor is more robust to changes in the couplings or potential shape within the constraints of the measured barrier distribution.

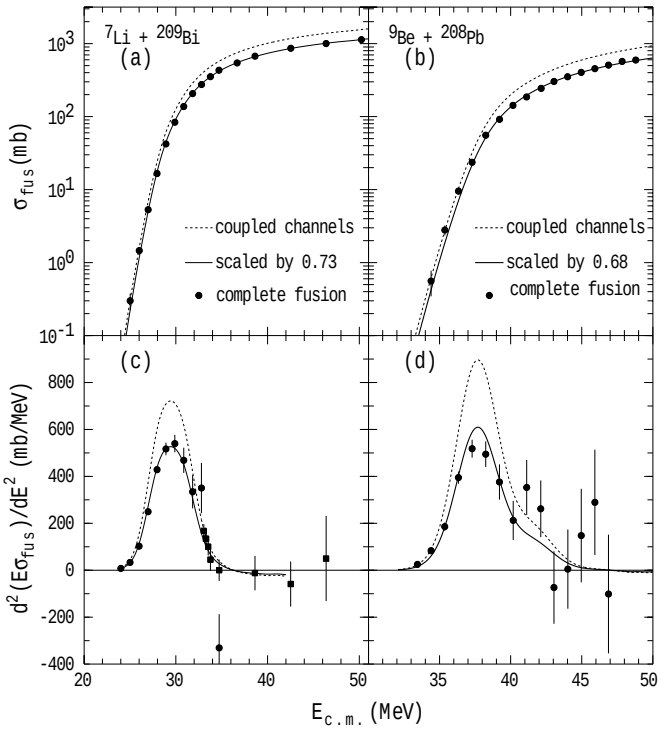

Fig. 4. The measured complete fusion cross-sections (top panels) and the experimental barrier distribution (bottom panels) for the reactions indicated. The dashed line is the result of a coupled-channels calculation which includes expected couplings to states in the target and projectile. The calculations do not include breakup effects. The full line is the same calculation scaled by factors as indicated, and gives a good representation of the complete fusion data.

The suppression of complete fusion at energies above the barrier, observed in both the reactions, is attributed to the reduction in the incident flux due to the large probability of ^{7}Li and ^{9}Be breaking up before they reach the fusion barrier. This picture is supported by the large incomplete fusion cross-sections which were observed in these experiments. It should be noted that complete fusion is here identified as the capture of all the charge of the projectile, and it includes breakup events where the breakup fragments are all captured by the target. In addition, in the case of the ^{9}Be induced reaction, the complete fusion cross-sections include events where ^{9}Be breaks up into two alpha-particles (or ^{8}Be) and a neutron, with the neutron escaping capture. Thus the experimental complete fusion yields underestimate the actual breakup probability.

The determination of the average barrier position has been crucial in obtaining a quantitative measure of the fusion suppression at above-barrier energies. Theoretical

models, which aim to describe the effect on fusion of the breakup of very weakly bound radioactive nuclei, should be able to explain these fusion data obtained for weakly bound *stable* nuclei, where halos are absent.

5 Conclusions

The insights into reaction dynamics which have occurred in recent years have in large part been due to the representation of fusion data in terms of a barrier distribution, and the increase in data quality which that requires. Further unexpected features of nuclear fusion are surely just waiting to be uncovered!

References

1. N. Rowley, G.R. Satchler, P.H. Stelson, Phys. Lett. B **254**, 25 (1991).
2. M. Dasgupta *et al.*, Annu. Rev. Nucl. Part. Sci. **48**, 401 (1998).
3. J.R. Leigh *et al.*, Phys. Rev. C **52**, 3151 (1995).
4. C.R. Morton, *et al.*, Phys. Rev. Lett. **72**, 4074 (1994).
5. A.M. Stefanini *et al.*, Phys. Rev. Lett. **74**, 864 (1995).
6. H. Timmers *et al.*, Phys. Lett. B **399**, 35 (1997).
7. D.J. Hinde *et al.*, Phys. Rev. Lett. **74**, 1295 (1995).
8. D.J. Hinde *et al.*, Phys. Rev. C **53**, 1290 (1996).
9. R. Vandenbosch, J.R. Huizenga, *Nuclear Fission* (Academic Press, New York, 1973).
10. C.H. Dasso, H. Esbensen, S. Landowne, Phys. Rev. Lett. **57**, 1498 (1986); A.B. Balantekin, P.E. Reimer, Phys. Rev. C **33**, 379 (1986); N. Rowley *et al.*, Phys Lett. B **314**, 179 (1993).
11. A.J. Sierk, Phys. Rev. C **33**, 2039 (1986).
12. B.B. Back *et al.*, Phys. Rev. C **32**, 195 (1985).
13. W.Q. Shen *et al.*, Phys. Rev. C **36**, 115 (1987).
14. S. Mitsuoka *et al.*, Phys. Rev. C **62**, 054603 (2000).
15. K. Nishio *et al.*, Phys. Rev. C **62**, 014602 (2000).
16. H.A. Kramers, Physica VII **4**, 284 (1940).
17. V.M. Strutinsky, Phys. Lett. B **47**, 121 (1973).
18. C. Gregoire, C. Ngô, B. Remaud, Phys. Lett. B **99**, 17 (1981).
19. A. Gavron *et al.*, Phys. Rev. Lett. **47**, 1255 (1981); **48**, 835(e) (1982).
20. D.J. Hinde *et al.*, Phys. Rev. C **60**, 054602 (1999).
21. H.A. Weidenmüller, Z. Jing-Shang, Phys. Rev. C **29**, 879 (1984).
22. K.T. Lesko *et al.*, Phys. Rev. C **27**, 2999 (1983).
23. C.R. Morton *et al.*, Phys. Rev. C **62**, 024607 (2000).
24. C.R. Morton *et al.*, Phys. Lett. B **481**, 160 (2000).
25. D. Vorkapić, B. Ivanišević, Phys. Rev. C **52**, 1980 (1995).
26. J.P. Lestone *et al.*, Phys. Rev. C **56**, R2907 (1997).
27. M. Dasgupta *et al.*, Phys. Rev. Lett. **82**, 1395 (1999).
28. M. Dasgupta *et al.*, *Proceedings of the Workshop on Fusion Dynamics at the Extremes, Dubna, 2000* (World Scientific, 2001).